

Can We Reduce SPECT Acquisition Time Using MAP-EM Reconstruction?

Uygar Tuna^{*1}, Antti Sohlberg², Ulla Ruotsalainen³

^{1,3}Department of Signal Processing, Tampere University of Technology, BioMediTech,
P.O. BOX 533, FIN-33101, Tampere, Finland

²Laboratory of Clinical Physiology and Nuclear Medicine, Joint Authority for
Päijät-Häme Social and Health Care, Lahti, Finland

^{*1}uygar.tuna@tut.fi; ²antti.sohlberg@phsotey.fi; ³ulla.ruotsalainen@tut.fi

Abstract-The aim of this study was to investigate: could the number of projection angles, and thus the total acquisition time be reduced using maximum a posteriori expectation maximization (MAP-EM) method without loss in the quality of the reconstructed images? In this study, we evaluate the sequentially applied MAP-EM method in which the amount of regularization is reduced step-by-step during the reconstruction process. The method was used for the reconstruction of the SPECT data with few projection angles and at low count levels. We assessed the MAP-EM method with three different spatial domain regularizers: (1) Median filter, (2) L-filter and (3) Block-Matching and 3D filter. The performance of the MAP-EM method was examined with numerical cardiac phantom and real patient data. We used a broad test dataset with different amount of projection angles at different count levels. The volumes reconstructed with the MAP-EM (with different regularizers) were compared to the images reconstructed with the maximum likelihood expectation maximization (MLEM) method. In addition to the visual evaluations, we gave comparisons using the contrast ratio and coefficient of variation measures. We also examined the reconstructed images via profiles drawn through the cardiac region. The images reconstructed with the sequentially applied MAP-EM method were visually very good and showed hardly any visual differences for most of the cases. The quantitative evaluations showed that for all cases, the reconstructed images were improved with the MAP-EM reconstruction method compared to the MLEM. For certain range of counts depending on the study and scanner properties, collecting the counts into fewer projection angles posed advantage on collecting the same amount of counts into more projection angles. With the inclusion of the sequential application of the regularization filter in the MAP-EM method, it is possible to reduce SPECT acquisition time down to certain levels depending on the collected amount of counts and numbers of projection angles.

Keywords- *Analytical Reconstruction; Block Matching and 3D Filtering; Bone Scan; Contrast Ratio; Few Angle Projection; Filtered Backprojection; Ill-Posed; Incomplete Sinogram; Inverse Problem; Maximum Likelihood Expectation Maximization; Median Filtering; Iterative Statistical Methods; Short-Duration Scan; Sparse Sinogram; Spatial Resolution*

I. INTRODUCTION

Recovering the unknown spatial distribution from a set of projection data (sinogram) obtained from scanner is image reconstruction in the field of medical image processing. The image reconstruction is an ill-posed inverse problem for the real tomographic data acquisitions in which finite number of projections can be taken at certain angles. As the projections are acquired from limited angle configuration and at low count levels, this inverse problem becomes significantly more ill-posed.

Reduced duration of scan time in nuclear medicine imaging is desired in order to increase the number of patients to be scanned during a working day. The duration of the data acquisition in nuclear medicine imaging such as single photon emission computed tomography (SPECT) can be achieved in two ways: (1) Reducing the number of acquired projection angles while keeping the duration of the data acquisition per projection angle the same, (2) Reducing the duration of the data acquisition per projection angle while keeping the number of acquired projection angles the same. Assuming that the radiation dose injected to the patient stays the same, the amount of the collected counts depends on the duration of the SPECT scan. For the same amount of collected counts, while the first way of collecting counts favors better sampling in radial direction (*i.e.* collecting less projection angles but relatively higher counts per projection angle), the second approach favors better angular sampling (*i.e.* collecting more projection angles but relatively lower counts per projection angle). These two ways for reducing the scan duration pose a trade-off between less projection angles at higher count levels and more projection angles at lower count levels.

The image reconstruction can be performed either using analytical methods (*e.g.* filtered backprojection, FBP) or iterative statistical methods (*e.g.* expectation maximization, EM, based methods). The analytical methods which require complete projection data obligate the gap-filling methods for the missing projection data. The compensation methods for the missing parts in the projection data have been published in the literature [1, 2]. However, these methods cannot successfully compensate for the missing data if the whole projection vector (*i.e.* the projection data taken at same angle) is missing as in the limited angle or sparse tomography. Successful solution for the severely ill-posed inverse problems requires a priori information, regularization and system matrix modeling to be engaged in the reconstruction process. The analytical reconstruction methods are not suitable for the sparse angle projection data as they are not flexible for the inclusion of the a priori information and the regularization as well as the system matrix modeling [3]. Therefore, iterative statistical methods

pose advantage over the analytical methods as they can be further modified in order to handle projection data acquired from sparse angle configuration. Regularization in iterative statistical methods is usually regarded as visually displeasing since the reconstructed images might exhibit additional blurring and loss of structures depending on the amount of regularization. Moreover, the quality of the reconstructed images might be highly dependent on the employed regularization filter. The sequential application of the regularization filters in the maximum a posteriori EM (MAP-EM) method (achieved by reducing the amount of regularization throughout the iterations) reduces the undesired effects of the regularizer in the reconstructed images.

Previously, we showed promising preliminary results of the sequentially applied EM method [4] regularized with Median (MED) filtering [5], L-filtering [5] and Block-matching and 3D (BM3D) filtering [6] with various kinds of incomplete projection data using numerical phantom data. The aim of this study was to assess this novel sequentially applied MAP-EM method with few projection angles and low count SPECT data in order to answer the question “Could the number of projection angles, and thus the acquisition time be reduced using sequentially applied MAP-EM method without loss in the quality of the reconstructed images?”.

II. MATERIALS AND METHODS

A. Experimental Dataset

1) Numerical Phantom Data:

We used the 3D numerical cardiac phantom ($128 \times 128 \times 128$) (Fig. 1) as the test data source. To simulate the data acquisition, the projection images (of the size 128×128) were generated from 64 angles over 180 making up $128 \times 64 \times 128$ (radial samples \times angular views \times slices) sinogram data. The test dataset was constructed from the projection data by scaling and contaminating Poisson noise. We performed simulations with the dataset at 5 different counts levels ($\sim 8 \times 10^6$, $\sim 4 \times 10^6$, $\sim 2 \times 10^6$, $\sim 1 \times 10^6$, $\sim 0.5 \times 10^6$ counts in the sinograms) for 3 different projection angles (64, 32 and 16 angles) making 15 different projection data.

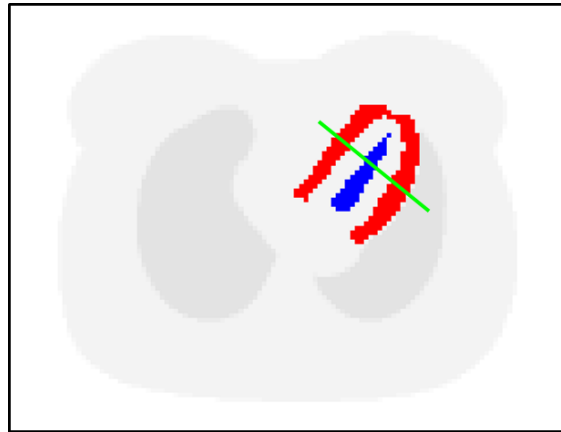


Fig. 1 Numerical cardiac phantom shown with regions of interests corresponding to heart wall (red region) and ventricle (blue region) which are used for contrast ratio (CR) and coefficients of variation (CoV) measures. The green line shows the direction from which the profile plots were obtained

2) Clinical Data:

We also evaluated the sequentially applied MAP-EM method with real patient bone SPECT data. The patient was injected 925 MBq of Tc-99m-MDP and scanned with the Siemens Symbia SPECT/CT scanner (Siemens Healthcare, Erlangen, Germany). 128×128 projection images were collected at 64 different angles distributed evenly in 360° acquisition (sparsely taken with an angular increment of 5.6250°). Hence, the acquired projection data were of the size $128 \times 64 \times 128$ (radial samples \times angular views \times slices) with 4.8 mm bin size. The duration of the acquisition was 20 sec. for each angle and $\sim 3 \times 10^6$ counts were collected in total. The projection data with 64 angular views is referred to as BONE_64 in the text. We modeled the acquisition with fewer projection angles and constructed the BONE_32 (at ~ 1.5 M counts) and BONE_16 (at ~ 0.75 M counts) datasets by using 32 and 16 projection angles drawn from the BONE_64 projection data.

B. Image Reconstruction

The projection dataset was reconstructed using the well-known maximum a posteriori expectation maximization (MAP-EM) reconstruction method. The method was modified such that it includes system matrix modeling for the missing projection bins and employs spatial domain regularization. The novel modification was achieved with the sequential application of the regularization step in the MAP-EM method. The block diagram of the sequentially applied MAP-EM method is given in Fig. 2. The one step late (OSL) algorithm including regularization and system matrix modeling for the unmeasured projection bins can be formulated as,

$$\lambda_j^{k+1} = \frac{\lambda_j^k}{\sum_i a_{ij} + \beta \left(\frac{\lambda_j^k - M_j}{M_j} \right)} \sum_i a_{ij} \left(\frac{y_{i \in \text{known_bins}}}{\sum_j a_{ij} \lambda_j^k} + J_{i \in \text{unknown_bins}} \right) \quad (1)$$

where λ_j^k and λ_j^{k+1} are the pixel values in the reconstructed images in current and next iterations, respectively, a_{ij} is the system matrix, β is the parameter controlling the amount of regularization in each iteration, y_j stands for the projection data, J_i is the vector of one modeling the unmeasured sinogram bins (marked as 1 in Fig. 2) and where M_j is the penalty reference calculated by using different spatial domain regularizers (marked as 2 in Fig. 2).

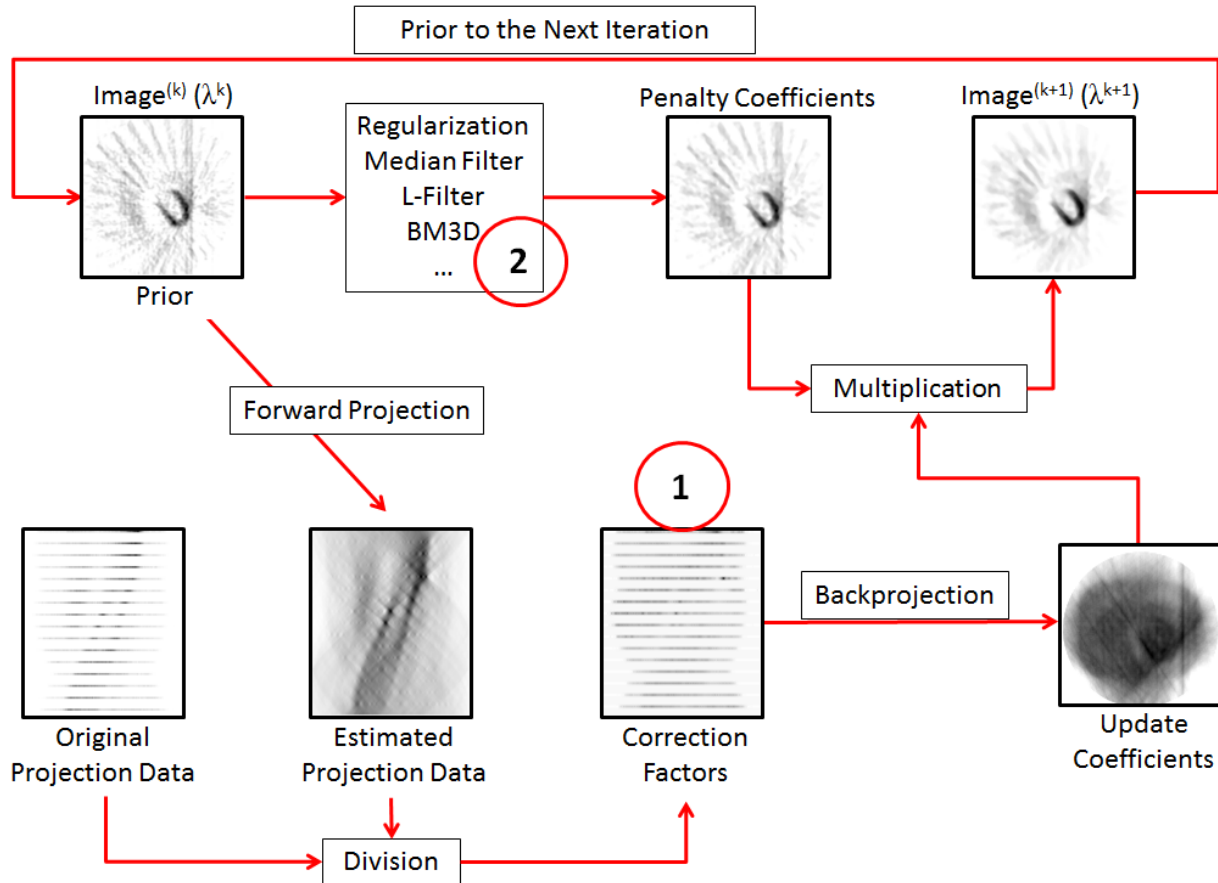


Fig. 2 Block diagram of the regularized MAP-EM method shown with the numerical cardiac phantom data. The method is initialized with the FBP reconstruction of the original projection data. The modifications are marked with as 1 and 2

The first modification done to the MAP-EM method is modeling the missing projection bins in the correction factors step which is marked as 1 in Fig. 2 and shown with the vector of ones for the unknown projection bins, J_i in the Equation (1). The correction factors hold the update information to be backprojected into spatial domain and to be applied to the image of the previous iteration. In the correction factors data, the correction factors which fall into the unknown projection bins are set to value 1. This setting lets the unknown projection bins vary throughout the iterations and converge to the correct values with the help of spatial domain regularization while the MAP-EM method tries to find the best match between the estimated and the original projection data.

The amount of the regularization in the MAP-EM method is defined by the parameter β ($0 < \beta < 1$) as in [5]. While β value of 1 corresponds full regularization, β value of 0 results in maximum likelihood expectation maximization (MLEM) method which does not employ without regularization. In this study, we applied regularization in the MAP-EM method sequentially by changing the β parameter throughout the iterations. We started the MAP-EM iterations with $\beta=1$. We reduced the β value linearly to 0.1 in 10 steps and performed a final step with $\beta=0.01$. This novel sequential application of the MAP-EM was performed to recover the blurring caused by the regularization filter (Fig. 3). On the other hand, in order to avoid having MLEM, the β value was not reduced to 0. Because, the MLEM iterations (*i.e.* $\beta=0$) would produce variations in the image and degrade the visual quality of the reconstructed images. The amount of spatial domain regularization (*i.e.* value for parameter β) was changed when the difference in the reconstructed images between the MAP-EM iterations was negligible (*i.e.* smaller than a pre-defined mean square error value). The criterion for changing the β value was decided experimentally.

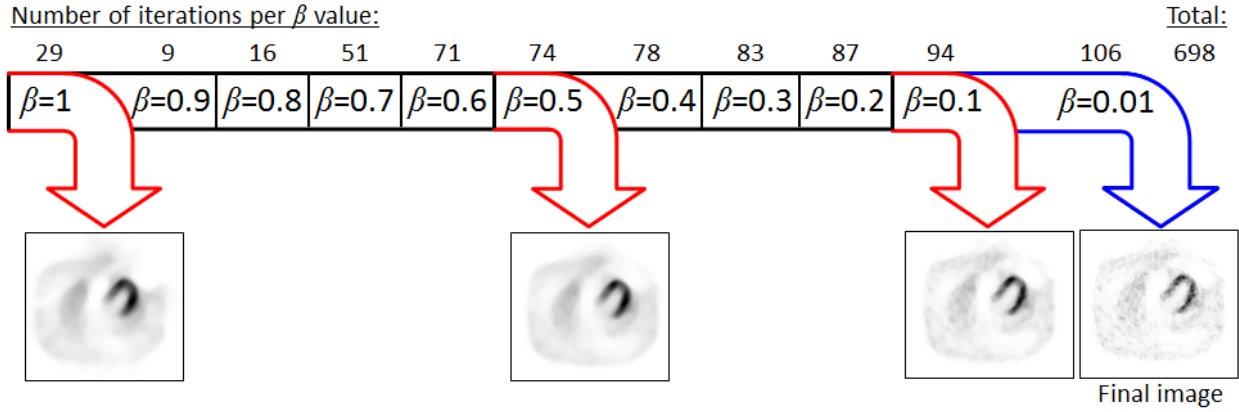


Fig. 3 The effect of sequentially reduced amount of regularization on the resulting image is shown with the numerical cardiac phantom data with 32 angles at $\sim 4M$ counts. The spatial domain regularizer was L-filter. The numbers of iteration per β value and the total number of iterations are also shown. The recovered resolution with the novel sequential application of the spatial domain regularizer are visualized by showing the intermediate images after $\beta=1$, $\beta=0.5$, $\beta=0.1$ and $\beta=0.01$ (final reconstructed image)

The second modification (marked as 2 in Fig. 2) was the usage of different spatial domain regularizers in the MAP-EM method. We employed three different spatial domain regularizers: (1) Median (MED) filter [5], (2) L-filter [5] and (3) Blockmatching and 3D (BM3D)¹ filter [6, 7]. MED and L filters, which were proposed as robust MLEM regularizers in [5], were applied in a 3×3 filtering window. MED filter returns the middle value of the ordered values within a filtering window as,

$$M_j = MED(\lambda^k; j). \quad (2)$$

L-filter outputs are a linear combination of the ordered values within the filtering window which can be formulated as,

$$M_j = L(\lambda^k; j) = \sum_{i \in N_j} a_i \lambda_{(i)}, \quad (3)$$

where $\lambda_{(i)}$ stands for the index of the ordered pixels and a_i represents the weight for the ordered pixels [5]. The weights used in the L-filter pose a compromise between mean and median filters. We used the weights for the L-filter as proposed in [5]. BM3D filter is an image denoising filter based on the collaborative filtering. The block diagram of the method is shown in Fig. 4. Collaborative filtering is performed in the 3D transform domain over the stacked (grouped) similar 2D fragments of the image (referred as blocks in Fig. 4). Previously, we showed that BM3D can be used for denoising both projection data and images [4, 8]. In this study, the BM3D filter was used as spatial domain regularizer. We used implementation of the BM3D filter as published in [7] with variance and smoothing parameters as 10^{-5} and 0.95, respectively. We also reconstructed the simulation dataset using the MLEM method (*i.e.* $\beta=0$ for MAP-EM method). We used 100 MLEM iterations in the reconstruction (similar as used in [9]). Furthermore, we used early stopping (10 MLEM iterations) which corresponds to low-pass filtering the reconstructed images. The sequentially regularized MAP-EM and MLEM iterations were initialized with the well-known analytical reconstruction method, filtered backprojection (FBP). We performed FBP with Hann filter (cut-off frequency with 1 cycle/pixel).

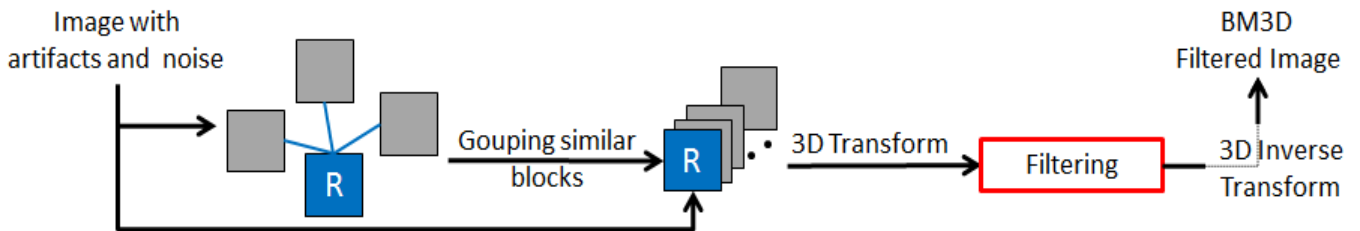


Fig. 4 Block diagram for the BM3D filtering method. The blue box (indicated with the letter R) is the reference block and the other gray colored boxes represent the blocks similar to the reference block

C. Contrast Ratio and Coefficient of Variation Evaluations

We assessed the performances of the regularizing filter using contrast ratio (CR) measure. CR measures the difference in the contrast between the target and background regions and can be formulated as,

¹<http://www.cs.tut.fi/foi/GCF-BM3D/>

$$CR = \frac{\bar{f}_{Target}(x, y, z) - \bar{f}_{Background}(x, y, z)}{\bar{f}_{Background}(x, y, z)}, \quad (4)$$

where $\bar{f}_{Target}(x, y, z)$ and $\bar{f}_{Background}(x, y, z)$ are the averaged intensity values in the selected target and background regions, respectively. We calculated the CR values with the numerical cardiac phantom data. We used the 3D regions for the heart wall (as the target region) and ventricle (as the background region). In Fig. 1, a slice of the numerical cardiac phantom is shown with the target (red region) and background (green region) regions. Moreover, no PVE correction was applied to the reconstructed images before CR calculations.

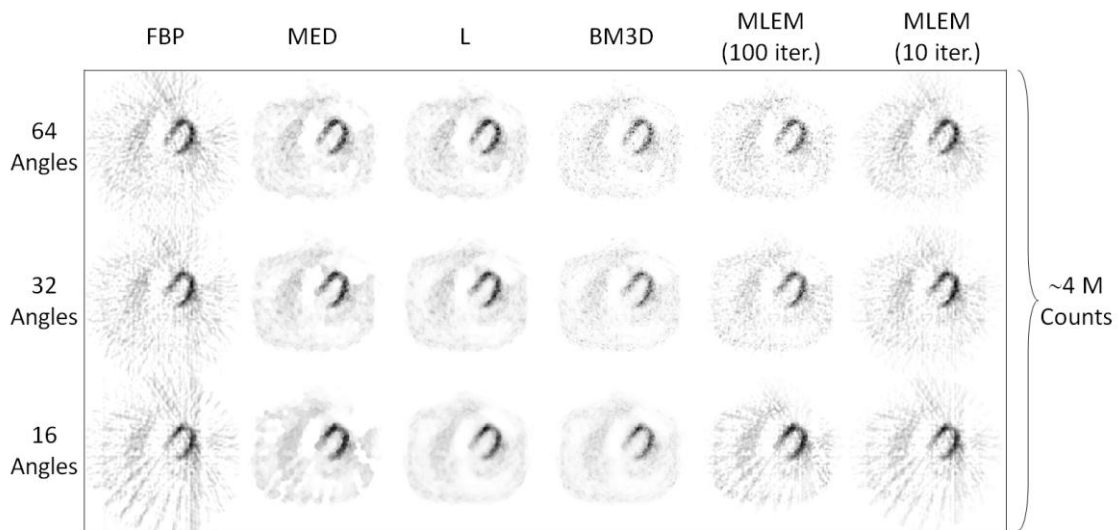
The coefficient of variation (CoV) measure was conducted in order to test the amount of variation in the target region of the reconstructed images. CoV can be formulated as,

$$CoV = \frac{\sqrt{\frac{1}{KLM} \sum_{x=1}^K \sum_{y=1}^L \sum_{z=1}^M (f_{Target}(x, y, z) - \bar{f}_{Target}(x, y, z))^2}}{\bar{f}_{Target}(x, y, z)}, \quad (5)$$

where $f_{Target}(x, y, z)$ and $\bar{f}_{Target}(x, y, z)$ correspond to the intensity value of the voxel in the region and the mean intensity value of all voxels in that region. We performed the CoV measure for the heart wall region (red region in Fig. 1) of the numerical cardiac phantom data.

III. RESULTS

In Fig. 5, we compare the results obtained from the numerical cardiac phantom sinogram data at ~4M, ~2M and ~1M counts. The images which are grouped together were reconstructed from the sinograms acquired within the same scan time. Regardless of the amount of the projection angles, the acquisition time for the sinograms from which the top group of images was obtained corresponds to 4 times longer than the bottom and 2 times longer than the middle group of images. It should be noted that, we assume that the radiation dose injected to the patient was the same. The visual quality of the images lying within the same group of images support our hypothesis as for certain cases collecting the data into fewer projection vectors results in images at visually better quality. For example, using 32 projection angles rather than 64 angles in the reconstruction (with MAP-EM method) resulted in higher visually quality (sharper image with less variation) images. Furthermore, in Fig. 6, we show the reconstructed images with the clinical SPECT bone scan data (BONE_64, BONE_32, and BONE_16). The reduced number of projection angles corresponds to the reduced number of counts in the sinograms as well as the reduced amount of scan time. We show the real patient images reconstructed from the sinogram data at ~3M, ~1.5M, and ~0.75M counts. The images reconstructed with MAP-EM method from the ~3M and ~1.5M data are at the same visual quality. In the reconstructed images with BONE_16 (~0.75M) data, the structures were still resolvable with a slight loss in the details (*i.e.* small targets). Both in Figs. 5 and 6, the MLEM method could not provide satisfactory results.



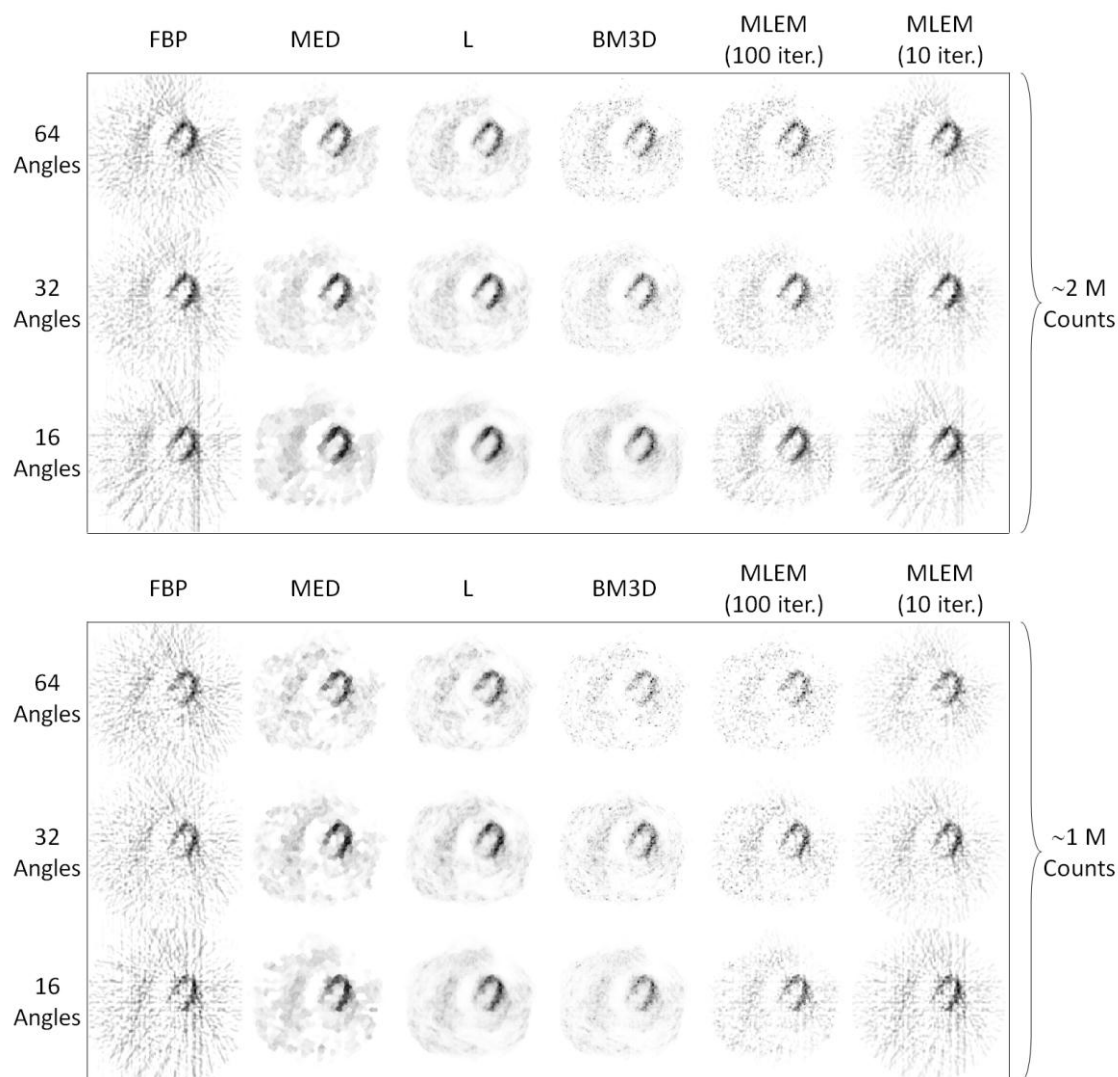
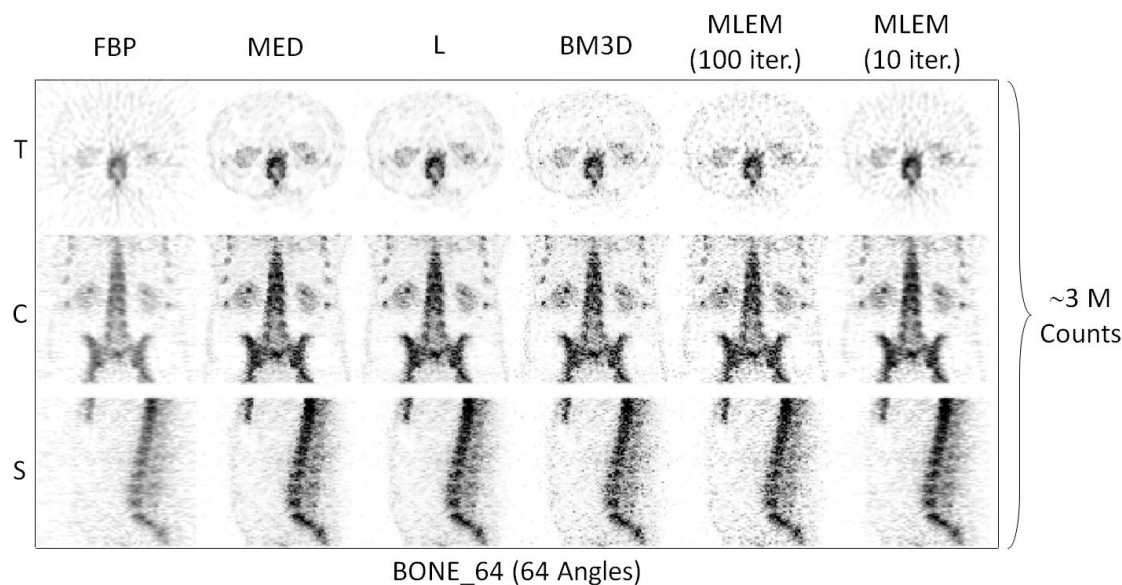


Fig. 5 Reconstructed images from the numerical cardiac phantom data. The rows correspond to the images reconstructed from the sinogram data with 64, 32 and 16 angles at ~4M, ~2M and ~1M counts. The acquisition times for the group of images in the bottom are 4 times less than the acquisition times for the group of images in the top and 2 times less than the acquisition times for the group of images in the middle for the same radiation dose injected to the patient. Columns show the sequentially applied MAP-EM method (with MED, L and BM3D filters) and MLEM method (after 100 iterations and 10 iterations) results after initialized with the shown FBP images. It should be noted that for certain cases, collecting the data into fewer projection angles poses advantage on collecting data into more projection angles



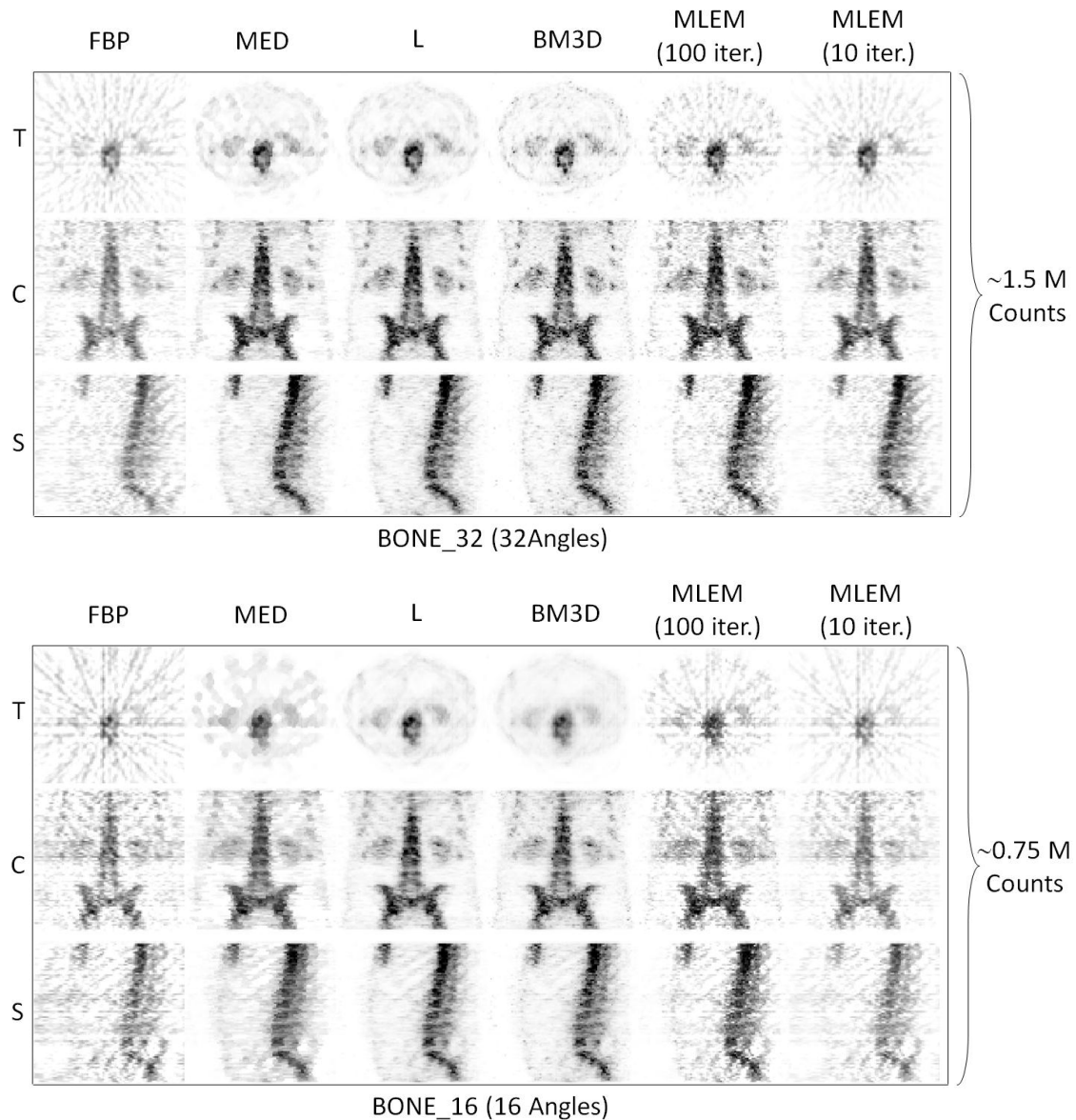


Fig. 6 Reconstructed images from the clinical bone SPECT data with different amount of projection angles (64, 32 and 16 projection angles) and consequently reduced scan durations. Labels T, C and S correspond to different orthogonal views of the reconstructed images, transaxial, coronal and sagittal views, respectively. The numbers of counts in the sinograms from which the images were reconstructed are also given. Columns show the sequentially applied MAP-EM method (with MED, L and BM3D filters) and MLEM method (after 100 iterations and 10 iterations) results after initialized with the shown FBP images

In addition to the visual evaluations, we assessed the reduced amount of scan duration, number of counts and number of projection angles quantitatively using contrast ratio (CR) and coefficient of variation (CoV) measures. In Fig. 7, the CR versus CoV curves calculated from the numerical cardiac phantom data is plotted. In the curves, the count levels correspond to the scan durations. Therefore, regardless of the amount of collected projection angles, the scan duration needed to acquire the data at $\sim 8\text{M}$ counts is 16 times longer than the time to acquire $\sim 0.5\text{M}$ counts. It should be noted that collecting data into 16 projection angles reduced the variation in the reconstructed image with the loss of contrast between the heart wall and the ventricle. Moreover, we observed that for the majority of the cases, increased number of collected counts resulted in lower CoV and higher CR values for certain amount of projection angles. Furthermore, for the counts between $\sim 1\text{M}$ and $\sim 4\text{M}$ (except the 16 projection angle cases), we observed that the CoV and CR values were improved when the same amount of counts were collected to fewer projection angles for all reconstruction cases (*i.e.* MAP-EM with MED, L, BM3D and MLEM). For example, collecting $\sim 4\text{M}$ counts into 32 projection angles resulted in lower CoV and higher CR values compared to collecting the same amount of counts into 64 projection angles. This phenomenon was observed for all reconstruction cases. Early stopping of MLEM method resulted in smoother images but the reduction in the contrast ratio was evident. In Fig. 8, we plot the profiles in the numerical cardiac phantom images reconstructed from the 32 angle projection data by using the MAP-EM with L filtering. The direction from which profiles were extracted is shown with the green line in Fig. 1. It should be noted that the drawn profiles were far from the central part of the field-of-view. We observed that the profiles are in agreement. Changing the counts in the acquired data did not have clear effect on the resolution but on the contrast between the heart wall, ventricle and the lungs.

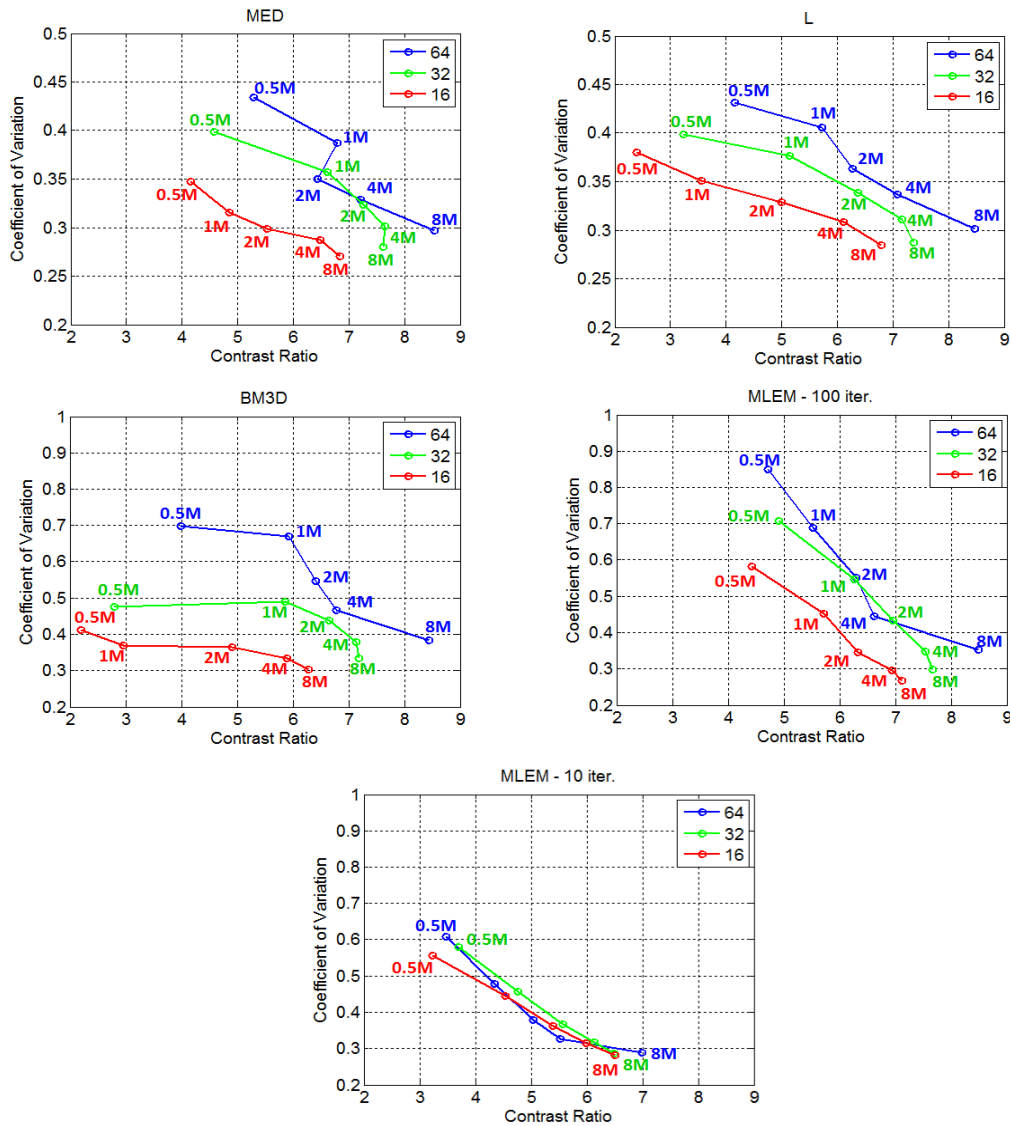


Fig. 7 CR versus CoV plots calculated from the numerical cardiac phantom data. Blue, green and red lines correspond to results from different amount of angles in the sinograms, 64, 32 and 16 angles, respectively. Moreover, the numbers at the data points in the curves stands for the count levels in the corresponding sinogram data

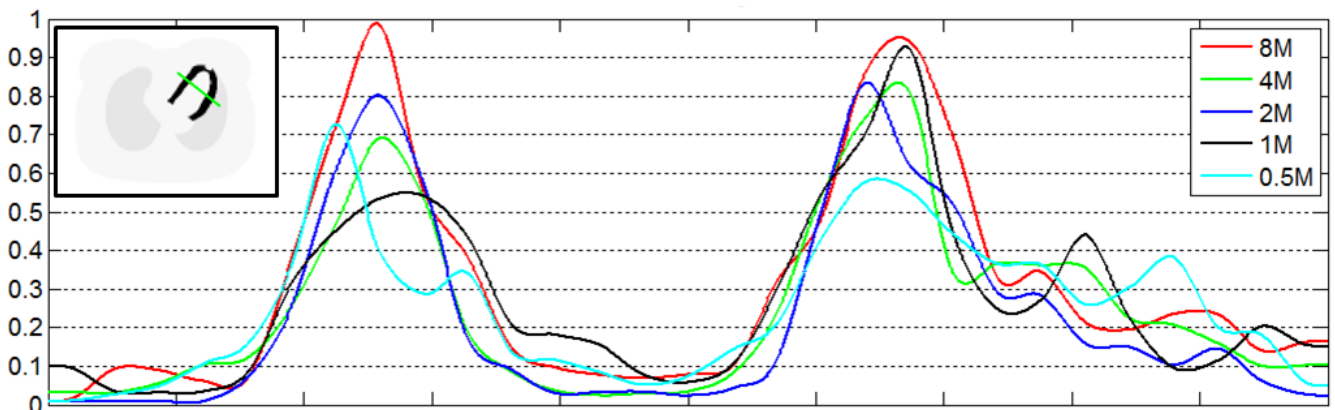


Fig. 8 Profile extracted from the reconstructed numerical cardiac phantom data with 32 angles using MAP-EM with L filter. The direction of the profile is shown with the green line in the legend image (also shown in Fig. 1). Different colored curves stand for the data at different count levels

IV. DISCUSSION

In SPECT, data acquisition is unfortunately quite time-consuming and thus the methods to reduce the acquisition time are continuously investigated. The acquisition time can be shortened by either using fewer projection angles or reducing the scan

duration per projection angle while keeping the number of projection angles the same. For example, the bone SPECT data (BONE_64) used in this study was acquired in approximately 21.3 min. The generated BONE_32 and BONE_16 data correspond to scans of 10.6 min. and 5.3 min. durations, respectively. Short-duration scans allow more patients to be scanned per day. Moreover, the reduced scan duration is important especially for the patients, who cannot tolerate long acquisition time and cannot stay still during the scan. The severe movement of the patients during the scan might cause the withdrawal of the scan and require the repetition of the study. The artifacts due to the long acquisition times such as motion artifacts would be reduced by shortening the duration of the scans.

In this study, we tested our previously developed sequentially applied MAP-EM method for the reconstruction of the short duration and sparse angle SPECT data. We compared three spatial domain regularization filters, MED, L, and BM3D filters. These regularizers are easy to implement and require only couple of parameters (window size for MED and L, weights for L, block size and smoothing parameters for BM3D filters) to be set. Moreover, the tested reconstruction method does not require any priori information. We evaluated the sequentially applied MAP-EM method with a broad test dataset consisting of numerical cardiac phantom and real patient data acquired from SPECT scanner. It is known that the regularization causes blurring, loss of details in the reconstructed images and the quality of the reconstructed images exhibits high dependency on the employed regularizer. With the sequential application of the MAP-EM method (*i.e.* decreasing the value of the β parameter gradually), the blurring effect of the regularization was decreased and the details in the reconstructed images became visible again. With the experimentally selected criterion for changing the β value, the regularized MAP-EM method was iterated approximately 700 times in total. This high iteration number is necessary in order to recover the artifacts related to the sparsity of the projection angles and to recover the blurring (simultaneously making the small structures more visible). On the other hand, high number of iterations is not feasible without regularization (*i.e.* MLEM where $\beta=0$). It is known that high number of iterations results in severe noise contamination in the reconstructed images with MLEM. One way to overcome this problem is the early stopping the MLEM reconstruction which corresponds to the low-pass filtering the reconstructed images. This poses a contradiction between the necessity of high number of iterations to reconstruct the sparse projection data and the noise handling during the image reconstruction process. Moreover, this fact shows the importance of the MAP-EM method in sparse tomography reconstruction.

In this study, we also showed the tradeoff between favoring better samples in radial direction (*i.e.* relatively more counts to be collected into relatively less projection angles) and in angular direction (*i.e.* relatively less counts to be collected into relatively more projection angles) during the data acquisition. We observed that for certain count levels, collecting the projection data into fewer projection angles resulted in higher quality reconstructed images with the sequentially applied regularized MAP-EM method. Under the light of this finding, more efficient SPECT scans could be planned. For example, the projection data could be collected firstly into 16 evenly distributed projection angles over 360° after which if the patient could tolerate longer scan time, the next other 16 evenly distributed projection angles could be acquired (making up 32 angles) and the scan could be continued as long as the patient could tolerate in order to collect further projection angles. This kind of step-by-step data acquisition protocol could shorten the duration of the scan, prevent withdrawal of the data due to the errors during the scan and make sure that the images can be reconstructed in any case.

The simulations with the sequentially applied regularized MAP-EM method were performed in 2D. However, the extension of the regularization filters to 3D is also possible. Moreover, the image reconstruction could be made faster with the usage of the ordered subsets during the reconstruction. On the other hand, using ordered subsets expectation maximization (OSEM) would employ very few projection angles which would result in noisier reconstructed images.

V. CONCLUSIONS

The sequentially applied regularized MAP-EM method with the spatial domain regularization filters can be used to obtain artifactfree reconstructed images from the projection data with few angles and at low counts. The assessments with real SPECT data showed that with the developed method, the duration of the SPECT examinations could be reduced significantly without loss in the quality of the reconstructed images. The method is easy to implement and use as the employed regularization filters require few parameters to be set.

ACKNOWLEDGMENTS

This work was supported by the Academy of Finland, (number: 129657, Finnish Programme for Centres of Excellence in Research 2006-2011) and by the Graduate School in Electronics, Telecommunication and Automation (GETA), Finland.

REFERENCES

- [1] U. Tuna, S. Peltonen, and U. Ruotsalainen. Gap-filling for the high-resolution PET sinograms with a dedicated DCT-domain filter. *Medical Imaging, IEEE Transactions on*, 29(3): 830–839, 2010.
- [2] Floris HP van Velden, Reina W Kloet, Bart NM van Berckel, Carla FM Molthoff, Adriaan A Lammertsma, and Ronald Boellaard. Gap filling strategies for 3-D-FBP reconstructions of high-resolution research tomograph scans. *Medical Imaging, IEEE Transactions on*, 27(7): 934–942, 2008.

- [3] R. Rangayyan, A. P. Dhawan, and R. Gordon. Algorithms for limited-view computed tomography: An annotated bibliography and a challenge. *Applied optics*, 24(23): 4000–4012, 1985.
- [4] U. Tuna, A. Pepe, and U. Ruotsalainen. Sequential regularized MLEM reconstruction method for incomplete sinograms. In *Nuclear Science Symposium and Medical Imaging Conference (NSS/MIC)*, 2011 IEEE, pp. 2553–2557. IEEE, 2011.
- [5] S. Alenius and U. Ruotsalainen. Generalization of median root prior reconstruction. *Medical Imaging, IEEE Transactions on*, 21(11): 1413–1420, 2002.
- [6] K. Dabov, A. Foi, V. Katkovnik, and K. Egiazarian. Image denoising by sparse 3-D transform-domain collaborative filtering. *Image Processing, IEEE Transactions on*, 16(8): 2080–2095, 2007.
- [7] K. Dabov, A. Foi, V. Katkovnik, and K. Egiazarian. Joint image sharpening and denoising by 3D transform-domain collaborative filtering. In *Proc. 2007 Int. TICSP Workshop Spectral Meth. Multirate Signal Process., SMMSP*, vol. 2007, 2007.
- [8] S. Peltonen, U. Tuna, E. Sanchez-Monge, and U. Ruotsalainen. PET sinogram denoising by Block-Matching and 3D filtering. In *Nuclear Science Symposium and Medical Imaging Conference (NSS/MIC)*, 2011 IEEE, pp. 3125–3129. IEEE, 2011.
- [9] T. Kangasmaa, A. Sohlberg, J.T. Kuikka, et al. Reduction of collimator correction artefacts with bayesian reconstruction in SPECT. *International Journal of Molecular Imaging*, 2011: 630813, 2011.